Converting transient chaos into sustained chaos by feedback control

Ying-Cheng Lai[1,2] and Celso Grebogi[2,3]
[1]*Department of Biomedical Engineering, The Johns Hopkins University School of Medicine, Baltimore, Maryland 21205*
[2]*Laboratory for Plasma Research, University of Maryland, College Park, Maryland 20742*
[3]*Department of Mathematics and Institute for Physical Science and Technology, University of Maryland, College Park, Maryland 20742*
(Received 19 August 1993)

A boundary crisis is a catastrophic event in which a chaotic attractor is suddenly destroyed, leaving a nonattracting chaotic saddle in its place in the phase space. Based on the controlling-chaos idea [E. Ott, C. Grebogi, and J. A. Yorke, Phys. Rev. Lett. **64**, 1196 (1990)], we present a method for stabilizing chaotic trajectories on the chaotic saddle by applying only small parameter perturbations. This strategy enables us to convert transient chaos into sustained chaos, thereby restoring attracting chaotic motion.

PACS number(s): 05.45.+b

I. INTRODUCTION

Boundary crises are catastrophic events that occur commonly in nonlinear dynamical systems [1]. In such a case, a chaotic attractor collides with its own basin boundary and is suddenly destroyed as a system parameter passes through the crisis value, leaving behind a chaotic saddle in the place of the original chaotic attractor in phase space. A chaotic saddle is nonattracting and has a dense set of "gaps." These gaps reflect a Cantor-set-like structure in both the stable and unstable foliations associated with the chaotic saddle [1,2]. As the parameter varies further beyond the crisis value, sizes of these gaps increase. Nonetheless, immediately after the crisis, the chaotic saddle resembles the original chaotic attractor since the sizes of the gaps are small. Physically, nonattracting chaotic saddles lead to transient chaos, namely, trajectories starting from most initial conditions wander around the chaotic saddle for a finite amount of time before settling into the final asymptotic state. The final state could be, for instance, an attractor at infinity.

To illustrate nonattracting chaotic saddles and the phenomenon of transient chaos, we use the Hénon map $(x_{n+1},y_{n+1})=(a-x_n^2+0.3y_n,x_n)$, where a is a parameter, as an example. Figure 1(a) shows a bifurcation diagram for the map, where the abscissa is the parameter a in a range (0.0,3.0) and the ordinate plots asymptotic values of the dynamical variable x. A boundary crisis occurs at $a_c \approx 1.426$ at which the chaotic attractor is destroyed. Hence, in Fig. 1(a), the asymptotic state of the map is attracting for $a < a_c$ and is nonattracting for $a > a_c$ [3]. The asymptotic x values plotted for $a > a_c$ are actually taken from a long orbit on the chaotic saddle. This orbit cannot be obtained by directly iterating the map, as we do for the case of $a < a_c$ where there are attractors, because numerical trajectories starting from almost all initial conditions except from a set of measure zero diverge from the chaotic saddle in a finite number of iterates. The orbit is computed by using a technique called the "proper interior maximum triple" (PIM-triple) method specially designed to keep trajectories on nonat-

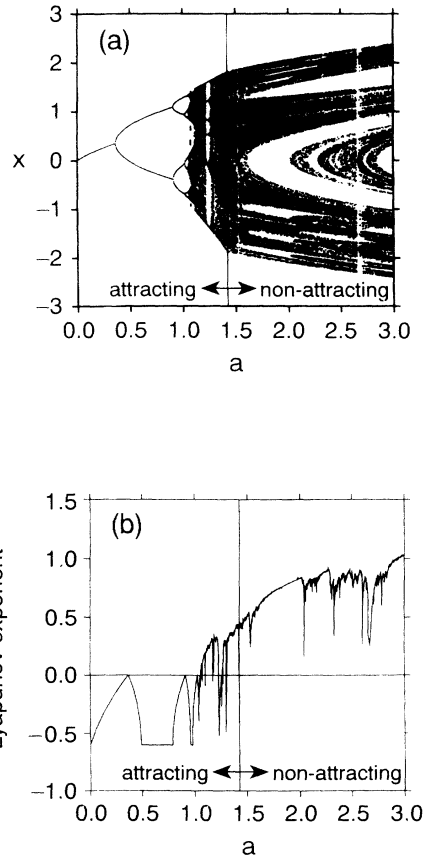

FIG. 1. (a) A bifurcation diagram and (b) a Lyapunov diagram of the Hénon map $(x,y)\rightarrow(a-x^2+0.3y,x)$ for $a\in[0.0,3.0]$. A boundary crisis occurs at $a_c \approx 1.426$ (indicated by the vertical dividing line in both figures). The asymptotic state of the map is attracting for $a < a_c$ and is nonattracting for $a > a_c$. At $a = a_c$, the chaotic attractor is destroyed, leaving a nonattracting chaotic saddle in the phase space. The asymptotic dynamical variables and the Lyapunov exponents for $a > a_c$ are calculated by using a long PIM-triple orbit. While the dynamical nature is fundamentally different for attracting and nonattracting motions, the asymptotic dynamical variables appear to be continuous around the crisis.

tracting chaotic saddles arising in two-dimensional maps or three-dimensional autonomous flows [4]. In Fig. 1(a), the most notable characteristic of the chaotic saddles for $a > a_c$ is the appearance of gaps as the parameter a passes the crisis value a_c. These gaps exist in all scales and they occupy a larger portion of the phase space as a increases far above a_c. Figures 2(a) and 2(b) show, in phase space, the chaotic attractor at $a = 1.4 < a_c$ and the chaotic saddle at $a = 1.5 > a_c$. Despite gaps on the chaotic saddle in Fig. 2(b), the motion on the chaotic saddle resembles that on the chaotic attractor in Fig. 2(a) when a is not far from a_c. This is also reflected in the Lyapunov diagram shown in Fig. 1(b), where we plot the largest Lyapunov exponent of attractors before the crisis and that of chaotic saddles after the crisis. The Lyapunov exponent exhibits no apparent characteristic change when a passes a_c.

Physically, trajectories in the neighborhood of chaotic attractors and chaotic saddles have different behavior. Trajectories starting from initial conditions in the basin of the chaotic attractor will stay on the attractor forever. For chaotic saddles, trajectories only stay near them for a finite amount of time. Figure 3 shows a time series of x_n for $a = 1.5$ [Fig. 2(b)], where the initial condition for the plotted trajectory is $(x_0, y_0) = (-1.711, 0.0)$. The lifetime of transient chaos is 288 iterates in this case. At time step $n = 289$, the trajectory escapes the chaotic saddle in a catastrophic way and maps to an attractor at negative infinity in subsequent iterates. There are practical applications in which one wishes to avoid catastrophic events such as this. One example is the so-called "voltage collapse" that occurs in electrical power systems [5]. For a particular class of voltage collapse, the phenomenology is that the power supply system breaks down suddenly after exhibiting complicated dynamical behavior resembling that of transient chaos (Fig. 3). Theoretical models suggest that for this class of voltage collapse, boundary crisis may be the culprit [6]. Therefore the conversion of a transient chaotic trajectory into a sustained chaotic or periodic trajectory would prevent voltage collapse in such cases. In this paper, we address the following question: when the crisis is inevitable and a chaotic attractor has been transformed into a chaotic saddle, can one restore stable chaotic motion by converting transient chaos into sustained chaos by applying only *small* perturbations to one of the accessible system parameters?

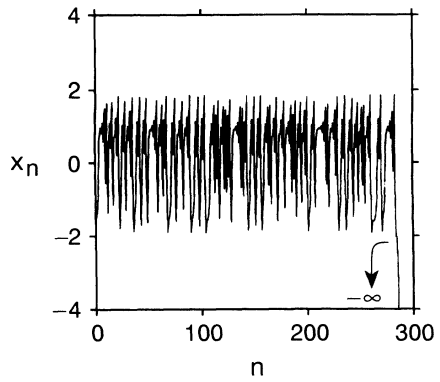

FIG. 3. A time series of x_n for the case of transient chaos at $a = 1.5$. The trajectory starts from the initial condition $(x_0, y_0) = (-1.711, 0.0)$. This trajectory wanders around the chaotic saddle of Fig. 2(b) for 288 iterates and escapes to an attractor at negative infinity in subsequent iterates.

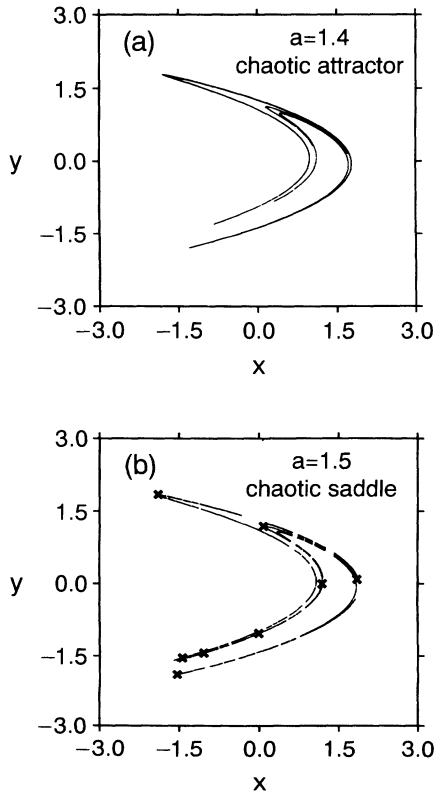

FIG. 2. (a) A chaotic attractor for the Hénon map at $a = 1.4$ and (b) a chaotic saddle at $a = 1.5$. The crosses in (b) denote the locations of a period-8 orbit embedded in the chaotic saddle.

Control of chaos using unstable periodic orbits embedded in a chaotic attractor has been proposed in Ref. [7]. The basic idea of the method is as follows. First one chooses an unstable periodic orbit embedded in the attractor, the one which yields the best system performance according to some criterion. Second, one defines a small region around the desired periodic orbit. Due to ergodicity of the chaotic attractor, the trajectory eventually falls into this small region. When this occurs, small judiciously chosen temporal parameter perturbations are applied to force the trajectory to approach the unstable periodic orbit. This method is extremely flexible because it allows for the stabilization of different periodic orbits, depending on one's needs, for the same set of nominal values of the parameter. This idea has since stimulated many theoretical investigations [8] and has been successfully applied in various physical [9], chemical [10], and biological [11] systems.

In this paper, we devise a scheme to restore sustained chaotic motion on the chaotic saddle by using the method of Ref. [7]. The key observation is that on the chaotic saddle there exist dense, though nonattracting, chaotic orbits. By selecting one such nonattracting orbit as the *reference orbit,* which can be constructed by using

the PIM-triple method, we can make other trajectories stay in the neighborhood of this reference orbit for as long as one wishes by applying small, judiciously chosen temporal parameter perturbations. In this sense, nonattracting trajectories in the neighborhood of the chaotic saddle are transformed into stable chaotic trajectories. This can indeed be achieved since there exist stable and unstable directions at each point of the reference orbit on the chaotic saddle. Hence, in principle, controlling a trajectory on the chaotic saddle is equivalent to stabilizing a long unstable periodic orbit as in Ref. [7]. We should mention that a method for stabilizing chaotic orbits on the attractor has been proposed and applied to the synchronization of two almost identical chaotic systems [12], and a method of creating desired chaotic orbits on a *chaotic attractor* has been implemented [13].

The organization of this paper is as follows. In Sec. II we discuss the method to stabilize a long chaotic orbit on the chaotic saddle. In Sec. III we present numerical results using the Hénon map and discuss the probability that a randomly chosen initial condition can be controlled. In Sec. IV we give conclusive remarks.

II. METHOD OF STABILIZING A CHAOTIC ORBIT

We consider a transient chaotic system that can be described by two-dimensional maps on the Poincaré surface of section

$$\mathbf{x}_{n+1}=\mathbf{F}(\mathbf{x}_n,p) , \tag{1}$$

where $\mathbf{x}_n \in \mathbb{R}^2$, p is an externally controllable parameter. For p values considered in this paper, we assume that Eq. (1) possesses only nonattracting chaotic saddles. We require the parameter perturbations to be small, i.e.,

$$|\Delta p| \equiv |p-p_0| < \delta , \tag{2}$$

where p_0 is some nominal parameter value and δ is a small number defining the range of parameter perturbations.

Let $\{\mathbf{y}_n\}$ $(n=0,1,2,\ldots,N)$ denote a long reference orbit on the chaotic saddle obtained by the PIM-triple method [4]. Now generate the orbit $\{\mathbf{x}_n\}$ to be stabilized around the reference orbit. Randomly pick an initial condition $\mathbf{x}_0$ and assume that the orbit point $\mathbf{x}_n$ $(n \geq 0)$ falls in a small neighborhood of the point $\mathbf{y}_k$ of the reference orbit on the chaotic saddle at time step n. Without loss of generality, we set $k=n$ on the reference orbit. In this small neighborhood, the linearization of Eq. (1) is applicable. We have, thus

$$\mathbf{x}_{n+1}(p_n)-\mathbf{y}_{n+1}(p_0)=\mathbf{J}[\mathbf{x}_n(p_0)-\mathbf{y}_n(p_0)]+\mathbf{K}\Delta p_n , \tag{3}$$

where $\Delta p_n = p_n - p_0$, $\Delta p_n \leq \delta$, $\mathbf{J}$ is the 2×2 Jacobian matrix, and $\mathbf{K}$ is a two-dimensional column vector,

$$\mathbf{J}=\mathbf{D}_{\mathbf{x}}\mathbf{F}(\mathbf{x},p)|_{\mathbf{x}=\mathbf{y}_n,p=p_0} , \quad \mathbf{K}=\mathbf{D}_p\mathbf{F}(\mathbf{x},p)|_{\mathbf{x}=\mathbf{y}_n,p=p_0} . \tag{4}$$

Without control, i.e., $\Delta p_n = 0$, the orbit $\mathbf{x}_i$ $(i=n+1,\ldots)$ diverges from the reference orbit $\mathbf{y}_i$ $(i=n+1,\ldots)$ exponentially. Our task is to program the parameter perturbations Δp_n in such a way that the trajectory $\mathbf{x}$ stays near the reference orbit on the chaotic saddle (or equivalently, $|\mathbf{x}_i-\mathbf{y}_i| \to 0|$) for subsequent iterates $i \geq n+1$.

For each reference orbit point on chaotic saddle, there exist both a stable and an unstable direction [14]. These directions can be calculated by using the numerical method of Ref. [14]. This numerical method, however, requires that the map be explicitly known. The calculated stable and unstable directions are stored together with the reference orbit, and they are used to compute the parameter perturbations applied at each time step. Let $\mathbf{e}_{s(n)}$ and $\mathbf{e}_{u(n)}$ be the stable and unstable directions at $\mathbf{y}_n$ and $\mathbf{f}_{s(n)}$ and $\mathbf{f}_{u(n)}$ be the corresponding contravariant vectors that satisfy $\mathbf{f}_{u(n)}\cdot\mathbf{e}_{u(n)}=\mathbf{f}_{s(n)}\cdot\mathbf{e}_{s(n)}=1$ and $\mathbf{f}_{u(n)}\cdot\mathbf{e}_{s(n)}=\mathbf{f}_{s(n)}\cdot\mathbf{e}_{u(n)}=0$. To stabilize $\{\mathbf{x}_n\}$ around $\{\mathbf{y}_n\}$, we require the next iteration of $\mathbf{x}_n$, after falling into a small neighborhood around $\mathbf{y}_n$, to lie on the stable direction at $\mathbf{y}_{(n+1)}(p_0)$, i.e.,

$$[\mathbf{x}_{n+1}-\mathbf{y}_{(n+1)}(p_0)]\cdot\mathbf{f}_{u(n+1)}=0 . \tag{5}$$

Substituting Eq. (3) into Eq. (5), we obtain the following expression for the parameter perturbation:

$$\Delta p_n = \frac{\{\mathbf{J}[\mathbf{x}_n-\mathbf{y}_n(p_0)]\}\cdot\mathbf{f}_{u(n+1)}}{-\mathbf{K}\cdot\mathbf{f}_{u(n+1)}} . \tag{6}$$

It is understood in Eq. (6) that if $\Delta p_n > \delta$, we set $\Delta p_n = 0$.

III. NUMERICAL RESULTS FOR THE HÉNON MAP

Figures 4(a) and 4(b) show an example of applying our algorithm to the chaotic saddle of the Hénon map shown in Fig. 2(b). We use a reference orbit on the chaotic saddle of length $N=10\,000$. The maximally allowed parameter perturbation is $\delta=0.01$ and the size of the small neighborhood around each point on the reference orbit is chosen to be $\epsilon=0.005$. We can choose both δ and ϵ arbitrarily, as long as they are small. We start the trajectory to be stabilized with initial condition $(x_0,y_0)=(0.5,-0.1)$. After four initial iterates, the trajectory falls into the neighborhood of a point of the reference orbit $[(x,y)\approx(-1.8393,1.8387)]$. When this occurs, parameter control based on Eq. (6) is turned on to stabilize the trajectory around the reference orbit. The controlled trajectory in the phase space is shown in Fig. 4(a). Figure 4(b) shows values of the parameter perturbations applied at subsequent time steps. Numerically, the controlled trajectory rapidly converges to the reference orbit. After a few iterates, the parameter perturbations required become extremely small (around 10^{-10}). Figures 4(a) and 4(b) thus demonstrate the applicability of the method of Ref. [7] for converting transient chaos into sustained chaos in dynamical systems. Note that, however, not every randomly chosen initial condition can be controlled. A fraction of trajectories starting from initial conditions in a square region defined by $-3 \leq x \leq 3$ and $-3 \leq y \leq 3$ escape to infinity without even getting closer to the chaotic saddle. Those initial conditions are, therefore, uncontrollable.

The probability that a randomly chosen initial condi-

tion can be controlled, $P(N,\epsilon)$, depends both on the length of the reference orbit N and the size ϵ of the small region around each reference point. Figure 5(a) shows the $P(N,\epsilon)$ versus N curve, where $\epsilon=0.01$. This curve is calculated by varying N systematically and randomly choosing 10^4 initial conditions with uniform probability distribution in the region $(-3\leq x\leq 3, -3\leq y\leq 3)$ for each fixed N value. The probability is given by the ratio between the number of initial conditions that approach the reference orbit before escaping to infinity and the total number of initial conditions chosen (10^4). For small N values, say $N<800$, $P(N,\epsilon)$ increases approximately linearly. The reason is that the probability that a trajectory enters the neighborhood of the chaotic saddle is approximately proportional to the total area of the small circles surrounding all the reference orbit points. This area is approximately $\pi\epsilon^2 N$ when overlaps between neighboring circles are small. As N increases further, the overlaps between neighboring circles become significant, thereby causing $P(N,\epsilon)$ to saturate. In fact, when $N>1000$, $P(N,\epsilon)$ increases very slowly. When N is larger than 10^4, $P(N,\epsilon)>0.66$ for the chaotic saddle in Fig. 2(b). The relation between $P(N,\epsilon)$ and ϵ for fixed $N=8000$ is shown in Fig. 5(b), which can roughly be fitted by $P(N,\epsilon)\sim\log\epsilon$. This is very different from the power-law scaling relation $P\sim\epsilon^{\gamma}$ predicted for the case of stabilizing short unstable periodic orbit on the chaotic saddle, where γ is a scaling exponent determined from the stable and unstable Lyapunov exponents associated with the periodic orbit [7,15,16]. The reason is that such a power-law scaling is valid only in the limit $\epsilon\rightarrow 0$ [7,15]. When the length of the target periodic orbit is small, such as the examples in Refs. [7,15,16], this power law can be observed for numerically suitable values of ϵ. When the length of the target orbit becomes large, such as our case of controlling a long reference chaotic orbit, the dependence of $P(N,\epsilon)$ on ϵ is much weaker. This is again due to the overlap of neighboring circles surrounding the reference orbit. When these overlaps are significant, increasing ϵ will not substantially increase $P(N,\epsilon)$. The power-law scaling relation would be realized when ϵ is extremely small, which is, however, numerically difficult to achieve for long chaotic orbits.

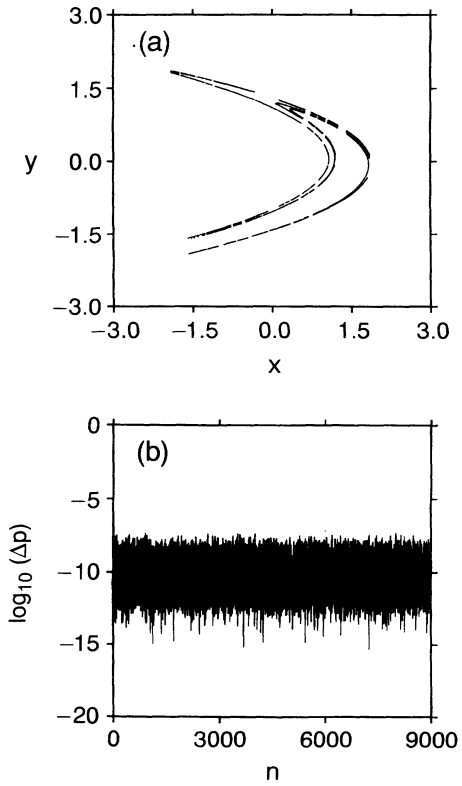

FIG. 4. (a) A restored sustained chaotic trajectory for $a=1.5$. (b) The time-dependent parameter perturbations applied to maintain the sustained chaotic motion in (a). Generally, the controlled trajectory rapidly converges to the chaotic saddle of Fig. 2(b). The required parameter perturbations are extremely small (around 10^{-10}) after a few controlling steps.

IV. CONCLUSIONS

In this work we have devised a scheme to convert transient chaos into sustained chaos by applying small perturbations to a system parameter. Our method is based on

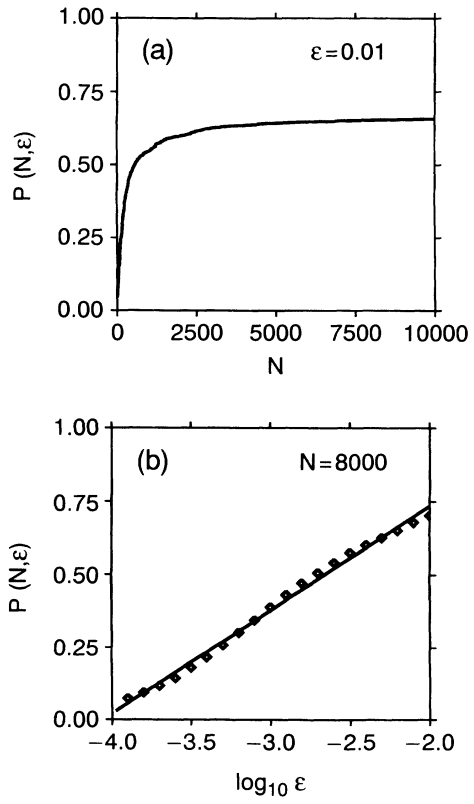

FIG. 5. (a) For fixed $\epsilon=0.01$ (the radius that defines the controlling neighborhood), the probability $P(N,\epsilon)$ that a randomly chosen initial condition can be stabilized around the chaotic saddle of Fig. 2(b) versus N, the length of the reference orbit. This probability increases initially with N and saturates for large N. The asymptotic value of $P(N,\epsilon)$ is approximately 0.66. (b) For fixed $N=8000$, $P(N,\epsilon)$ versus ϵ curve. This relation is approximately $P(N,\epsilon)\sim\log_{10}\epsilon$.

the idea of Ref. [7]. The novel feature is that we explicitly use the geometrical structure, i.e., stable and unstable directions, along a long reference orbit on the chaotic saddle to achieve the control. Our strategy thus allows us to restore sustained chaotic motion, thereby avoiding the catastrophic destiny of most orbits in the neighborhood of the chaotic saddle.

As a natural extension, our method can be applied to effectively stabilize unstable periodic orbits embedded in the chaotic saddle, such as the periodic-8 orbit shown in Fig. 2(b). Randomly pick an initial condition in the region of the figure; the goal is to stabilize the trajectory resulting from this initial condition in the neighborhood of the unstable period-8 orbit before the trajectory escapes to infinity. In a previous method [15], one chooses an ensemble of initial conditions, some of them enter the neighborhood of the target periodic orbit and can be controlled. In general, the probability that a randomly chosen initial condition is controlled is quite low because only a tiny fraction of trajectories enters the neighborhood of the desired periodic orbit. Nonetheless, we know that a dense chaotic orbit on the chaotic saddle comes arbitrarily close to the desired unstable periodic orbit [4]. The probability that a randomly chosen initial condition approaches a long reference orbit on the chaotic saddle is clearly much greater than the probability to enter the neighborhood of the desired unstable periodic orbit before it escapes the chaotic saddle. By stabilizing a trajectory around the long reference orbit on the chaotic saddle and then switching to stabilize it around the desired periodic orbit, we can *substantially* increase the probability that a trajectory can be controlled. In fact, by using a reference orbit of length about 1000, a factor of more than 10 increase in the probability of control has been achieved [17]. The longer the length of the reference chaotic orbit is, the larger this probability can be, as shown in Fig. 5(a).

Finally, we remark that the algorithm presented in this paper applies well when the system's equations are known. In experiments it is usually the case that only a measured time series is available. It is then necessary to use the delay-coordinate embedding technique [18] to extract quantities required to compute the parameter perturbations, such as the stable and unstable directions along a reference orbit. While calculating such quantities for low-periodic orbits embedded in a chaotic attractor is relatively easy to achieve [7,19], it is not clear at present that this may be possible for a long reference orbit embedded in a chaotic saddle. Therefore there is currently no assurance that our technique can be applied to real experimental systems in which the equations are not available. Nonetheless, we hope that the method of this paper will stimulate work on controlling transient chaos in experiments.

ACKNOWLEDGMENTS

We thank Tamás Tél for valuable discussions. This work was supported by DOE (Office of Scientific Computing, Office of Energy Research).

[1] C. Grebogi, E. Ott, and J. A. Yorke, Phys. Rev. Lett. **48**, 1507 (1982); Physica D **7**, 181 (1983).

[2] Y. C. Lai, C. Grebogi, and J. A. Yorke, in *Applied Chaos,* edited by J. H. Kim and J. Stringer (Wiley, New York, 1992), Chap. 19.

[3] There can be periodic attractors (sinks) even for $a > a_c$. However, the basins of those sinks are very small. We therefore exclude those sinks in our discussion. For a rigorous discussion concerning the nature of those periodic sinks, see L. Tedeschini-Lalli and J. A. Yorke, Commun. Math. Phys. **106**, 635 (1985), and references therein.

[4] H. E. Nusse and J. A. Yorke, Physica D **36**, 137 (1989).

[5] *Voltage Stability of Power Systems: Concepts, Analytical Tools and Industry Experience,* edited by Y. Mansour (IEEE, New York, 1990).

[6] H. Wang, E. H. Abed, and A. M. A. Hamdan (unpublished); H. Wang and E. H. Abed (unpublished); E. H. Abed, H. Wang, and R. C. Chen, Physica D (to be published).

[7] E. Ott, C. Grebogi, and J. A. Yorke, Phys. Rev. Lett. **64**, 1196 (1990); and in *Chaos: Soviet-American Perspectives on Nonlinear Science,* edited by D. K. Campbell (American Institute of Physics, New York, 1990).

[8] F. J. Romeiras, C. Grebogi, E. Ott, and W. Dayawansa, Physica D **58**, 165 (1992); U. Dressler and G. Nitsche, Phys. Rev. Lett. **68**, 1 (1992); D. Auerbach, C. Grebogi, E. Ott, and J. A. Yorke, *ibid.* **69**, 3479 (1992); Y. C. Lai, M. Ding, and C. Grebogi, Phys. Rev. E **47**, 86 (1993).

[9] W. L. Ditto, S. N. Rauseo, and M. L. Spano, Phys. Rev. Lett. **65**, 3211 (1990); J. Singer, Y.-Z. Wang, and H. H. Bau, *ibid.* **66**, 1123 (1991); A. Azevedo and S. M. Rezende, *ibid.* **66**, 1342 (1991); E. R. Hunt, *ibid.* **67**, 1953 (1992); R. Roy, T. W. Murphy, Jr., T. D. Maier, and Z. Gills, *ibid.* **68**, 1259 (1992); C. Reyl, L. Flepp, R. Badii, and E. Burn, Phys. Rev. E **47**, 267 (1993).

[10] B. Peng, V. Petrov, and K. Showalter, J. Chem. Phys. **95**, 4957 (1991).

[11] A. Garfinkel, W. L. Ditto, M. L. Spano, and J. Weiss, Science **257**, 1230 (1992).

[12] Y. C. Lai and C. Grebogi, Phys. Rev. E **47**, 2357 (1993).

[13] N. J. Mehta and R. M. Henderson, Phys. Rev. A **44**, 4861 (1991).

[14] Y. C. Lai, C. Grebogi, J. A. Yorke, and I. Kan, Nonlinearity **6**, 779 (1993).

[15] T. Tél, J. Phys. A **24**, L1359 (1991).

[16] Y. C. Lai, T. Tél, and C. Grebogi, Phys. Rev. E **48**, 709 (1993).

[17] Y. C. Lai, C. Grebogi, and T. Tél, in *Towards the Harnessing of Chaos,* Proceedings of the 7th TOYOTA Conference (Elsevier, Amsterdam, in press).

[18] F. Takens, in *Dynamical Systems and Turbulence,* edited by D. Rand and L. S. Young, Lecture Notes in Mathematics Vol. 898 (Springer-Verlag, New York, 1981).

[19] W. L. Ditto, S. N. Rauseo, and M. L. Spano, Phys. Rev. Lett. **65**, 3211 (1990).

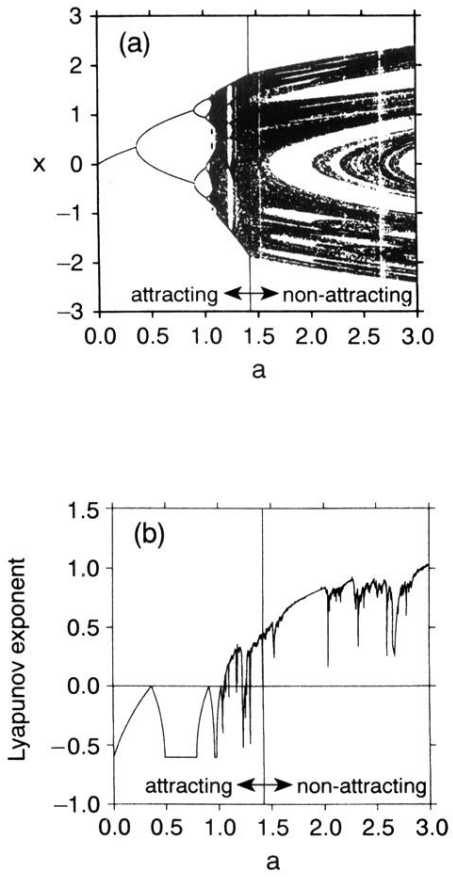

FIG. 1. (a) A bifurcation diagram and (b) a Lyapunov diagram of the Hénon map $(x,y)\rightarrow(a-x^2+0.3y,x)$ for $a\in[0.0,3.0]$. A boundary crisis occurs at $a_c\approx 1.426$ (indicated by the vertical dividing line in both figures). The asymptotic state of the map is attracting for $a<a_c$ and is nonattracting for $a>a_c$. At $a=a_c$, the chaotic attractor is destroyed, leaving a nonattracting chaotic saddle in the phase space. The asymptotic dynamical variables and the Lyapunov exponents for $a>a_c$ are calculated by using a long PIM-triple orbit. While the dynamical nature is fundamentally different for attracting and nonattracting motions, the asymptotic dynamical variables appear to be continuous around the crisis.